Ab initio calculation of lattice dynamics in FePd intermetallics

2008 J. Phys.: Condens. Matter 20 275208

(http://iopscience.iop.org/0953-8984/20/27/275208)

IOP PUBLISHING JOURNAL OF PHYSICS: CONDENSED MATTER

J. Phys.: Condens. Matter **20** (2008) 275208 (6pp) doi:10.1088/0953-8984/20/27/275208

Ab initio calculation of lattice dynamics in FePd intermetallics

Subhradip Ghosh

Department of Physics, Indian Institute of Technology Guwahati, Guwahati-781039, India

E-mail: subhra@iitg.ernet.in

Received 8 March 2008, in final form 12 May 2008
Published 3 June 2008
Online at stacks.iop.org/JPhysCM/20/275208

Abstract

The lattice dynamics of FePd and $FePd_3$ intermetallics have been investigated using an *ab initio* electronic structure method. The phonon dispersions and the contribution of each of the components to each branch of dispersion for three symmetry directions, along with the phonon densities of states, are calculated and compared with experiments. The force constants between various pairs of atoms in these intermetallics are obtained from first-principles calculations and the results are discussed based upon analysis of these data. A possible route to obtain force constants for disordered alloys from the intermetallics results is also discussed.

1. Introduction

Iron-based alloys and compounds have been subjected to an extensive amount of research lately because of their potential applications in shape-memory effects [1, 2], high-density magnetic recording media [3–5] and spintronics applications [6, 7]. Detailed knowledge of the various elementary excitations like the electron, the phonon and magnons is essential to understand the material properties of these alloys in their various ordered and disordered phases. A wealth of experimental results are available on Fe-based intermetallics and disordered alloys to help understand the microscopic origin behind various complex behaviors observed in these systems. On the theoretical side, compared to the amount of work available on electronic excitations and their possible significance in understanding and tailoring properties in these materials, there are fewer works on phonon excitations or understanding the lattice dynamics. Understanding the lattice dynamics is essential to understand the ordering behavior and its relation to many material properties of interest [8].

FePd alloys are interesting for the following reasons: first, Fe and Pd have different structures in their elemental phases while they form a single unique lattice upon alloying; second, they exhibit invar characteristics around the 3:1 stoichiometric composition; third, recent studies have identified the system as a potential candidate for magnetic media and shape-memory applications [1, 9, 10] due to strong magnetic anisotropy. There have been experimental investigations on the lattice dynamics and its coupling with magnetic ordering in disordered phases [11, 12], on the lattice dynamics in intermetallics $FePd_3$ [13] and FePd and estimation of vacancy formation enthalpy and migration enthalpy [14] which govern the diffusion and ordering kinetics. Results on the phonon spectrum, the densities of states and various thermodynamic parameters in these ordered intermetallics are therefore available. However, no theoretical investigation of lattice dynamics in these ordered intermetallics have yet been made. There are several theoretical works on the disordered phases of FePd [15] but all of them are based upon constructing model potentials and are therefore not parameter-free. Moreover, none of these studies could provide a microscopic understanding of the lattice dynamics based upon the complex interplay of forces between different pairs of species. It is very important to understand the interplay of these forces and their effects on the phonon spectrum when the same species is subjected to different environments due to a change in composition or the state of order. An estimation of this effect can be understood by looking at the variation of the force constants between various pairs of atoms under changing compositions or state of order. *Ab initio* electronic structure methods are the most reliable theoretical tools to obtain accurate information on the phonon spectra and material properties derivable from it. Since the calculations are independent of any adjustable parameter, they also provide accurate information on the force constants, thus facilitating the understanding of lattice dynamics from a microscopic point of view.

In this paper, we perform first-principles electronic structure calculations on the ordered intermetallics FePd and $FePd_3$ and study their lattice dynamics. We focus on the dispersion curves and the densities of states, their variations

with the changing composition and their comparison with experimental results. We try to gain some insight by looking at the variations of the force constants between various pairs of atoms with changing compositions and by analyzing the contribution of each type of atom to a given normal mode. To our knowledge, such a detailed analysis based upon the first-principles force constants and the contribution of each species to each normal mode has not been done on these systems. This analysis also helps us to understand the feasibility of modeling the variation of the force constant in disordered phases by using results on ordered intermetallics.

The paper is organized as follows. In section 2, we present the details of the first-principles calculations. In section 3, the results on dispersion curves, densities of states, force constants and the atom-specific contribution to each mode are presented and discussed. Section 4 summarizes the key aspects of this work and provides a future direction.

2. Methodology

First-principles Quantum Espresso code[1] has been used to calculate the lattice dynamics in FePd and $FePd_3$ systems. Quantum Espresso is based upon density functional perturbation theory (DFPT) [16]. DFPT is a density functional theory based linear response method to calculate the electronic structure and phonon excitations in condensed matter systems. In this method, the dynamical matrix which provides information on lattice dynamics of the system can be obtained from the ground-state electron charge density and its linear response to a distortion of the nuclear geometry. One of the greatest advantages of DFPT—as compared to other nonperturbative methods for calculating lattice dynamical properties of crystalline solids (such as the frozen-phonon or molecular dynamics spectral analysis methods)—is that within DFPT the responses to perturbations of different wavelengths are decoupled. This feature allows one to calculate phonon frequencies at arbitrary wavevectors avoiding the use of super-cells and with a workload that is independent of the phonon wavelength. In Quantum Espresso, the implementation of DFPT is done within the plane wave-pseudopotential framework [17].

The low temperature structures of FePd and $FePd_3$ are tetragonal $L1_0$ and cubic $L1_2$, respectively. The experimental lattice constants ($a = 7.285$ au for $FePd_3$; $a = 7.29$ au and $c = 7.07$ au for FePd) were used in our calculations. For the electronic structure and phonon calculations, ultra-soft pseudopotentials[2] with nonlinear core corrections [18] were used. PBE-96 spin-polarized generalized gradient approximation (GGA) functionals [19] were used for the exchange–correlation part of the potential. GGA functionals were chosen because of their better capability in calculating ground-state properties. The kinetic energy cut-off was taken to be 45 Ryd for $FePd_3$ and 55 Ryd for FePd. The Brillouin-zone integrations were carried out with Methfessel–Paxton [20] smearing. Special **k**-point meshes containing 70 **k**-points for $FePd_3$ and 540 **k**-points for FePd in the irreducible wedge were used. The smearing parameter used were 0.04 Ryd and 0.05 Ryd for $FePd_3$ and FePd, respectively. These parameters are found to yield phonon frequencies converged to within 5 cm^{-1}.

Once adequate convergence is achieved for the electronic structure, the phonon dispersion curves, the force constants and the phonon densities of states are obtained using the linear response. Within DFPT, the force constants are conveniently computed in reciprocal space on a finite **q**-point grid and Fourier transformation is employed to obtain the real-space force constants [21]. The number of unique real-space force constants and their accuracy depend upon the density of the **q**-point grids: the closer the **q**-points are spaced, the more accurate the force constants are. In this work, the dynamical matrix is computed on a mesh containing 20 **q**-points for $FePd_3$ and 30 **q**-points for FePd commensurate with the **k**-point mesh. Such choices of **q**-meshes enabled computation of force constants up to fifth neighbor for $FePd_3$ and up to fourth neighbor for FePd. The dispersion curves were calculated by diagonalizing the dynamical matrix and the densities of states (partial and average) were computed using Eyvaz Isaev's code which uses the tetrahedron scheme of zone integration [22]. The atom-specific contributions to each vibrational mode were obtained from the absolute values of the phonon eigenvectors.

3. Results and discussions

3.1. FePd

Figure 1 shows the dispersion curves of $L1_0$ FePd for three symmetry directions. Open circles are neutron scattering experimental results [14], plotted for comparison. In general the agreement between theory and experiment is fairly good with some exceptions. The biggest disagreement is observed for modes along $[\zeta\zeta\zeta]$, $\zeta = \frac{|\vec{q}|}{|\vec{q}_{\max}|}$, $\vec{q}$ is the wavevector. Here, for higher ζ values, the frequencies obtained from first-principles calculations are generally higher than the experimental ones for both acoustic and optical modes. The sole exception is the optical mode denoted as 5 where the frequencies obtained by first-principles are underestimated, thus producing a larger LO–TO gap than is observed in the experiment. This feature of first-principles GGA calculated frequencies being higher than the experimental ones is also seen for optical modes along $[\zeta\zeta 0]$. The densities of states display an overwhelmingly large contribution of Pd atoms throughout most of the frequency spectrum while Fe has major contribution in the smaller frequency regime only. This is in sharp contrast with the densities of states results obtained using experimental frequencies [14]. In the experimentally determined densities of states, the high frequency spectrum was dominated by Fe while the low frequency part was dominated by Pd. This is only to be expected because Fe, being the lighter atom, would vibrate with higher frequencies. Although we have got the peaks around 2 and 3 THz, around 4

[1] Quantum Espresso is a community project for high-quality quantum-simulation software, based on density functional theory, and coordinated by Paolo Giannozzi. See http://www.quantum-espresso.org/ and http://www.pwscf.org/.

[2] We used the pseudopotentials Fe.pbe-nd-rrkjus.UPF and Pd.pbe-nd-rrkjus.UPF from the http://www.quantum-espresso.org/ distribution.

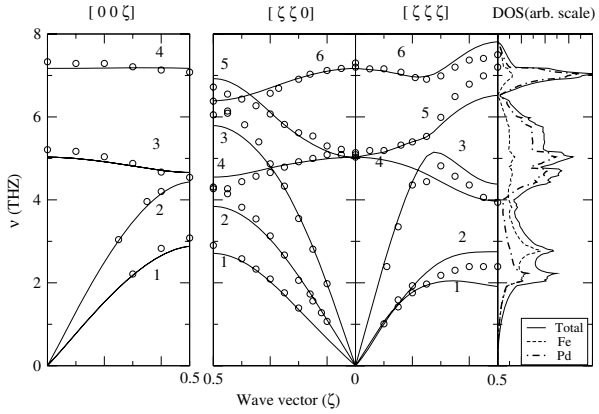

Figure 1. Dispersion curves (frequency ν versus reduced wavevector ζ) and phonon densities of states (partial and total) for FePd alloy. The open circles are the experimental data [14].

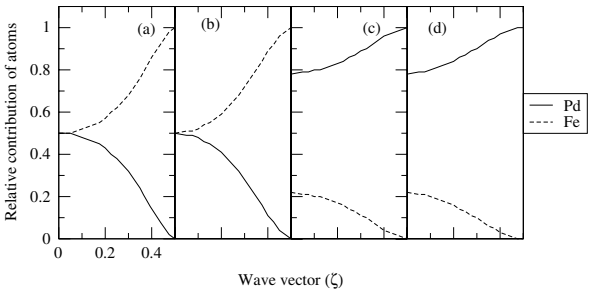

Figure 2. Relative contribution of Fe and Pd to each mode along [00ζ] in FePd. Parts (a)–(d) refer to modes 1–4, respectively, in figure 1.

and 5 THz, the relative intensities of the peaks are different from that of the experimental ones. The strongest peak is at around 7 THz, in agreement with the experiment, but in complete disagreement with the experiment it is dominated by Pd. We also see a sharp valley around 6 THz which is absent in the experimental curve. This sharp valley is due to a small contribution from Fe atoms around the frequency region.

In order to investigate this disagreement between theory and experiment, we have looked at the atom-specific contribution to each branch of phonon dispersion for all three symmetry directions. The results are displayed in figures 2–4. For all three symmetry directions, we find that the Pd atoms contribute much more than Fe atoms to the higher frequency optical modes. For the [$\zeta\zeta\zeta$] direction, apart from the lowest lying acoustic transverse mode, the Pd contribution significantly exceed the Fe contribution as ζ increases. Therefore, the overestimation of frequencies as seen in *ab initio* results, particularly along [$\zeta\zeta\zeta$], must be related to the dominant Pd contribution.

3.2. $FePd_3$

The dispersion curves and densities of states for $FePd_3$ are shown in figure 5. The neutron scattering results [13] are plotted for comparison. For this system, we do not have experimental data for most of the LO modes which are higher

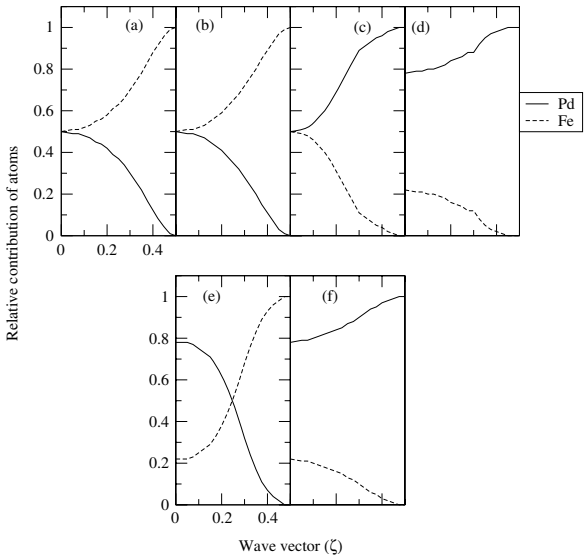

Figure 3. Relative contribution of Fe and Pd towards each mode along [$\zeta\zeta$0] in FePd. Parts (a)–(f) refer to the modes 1–6, respectively, in figure 1.

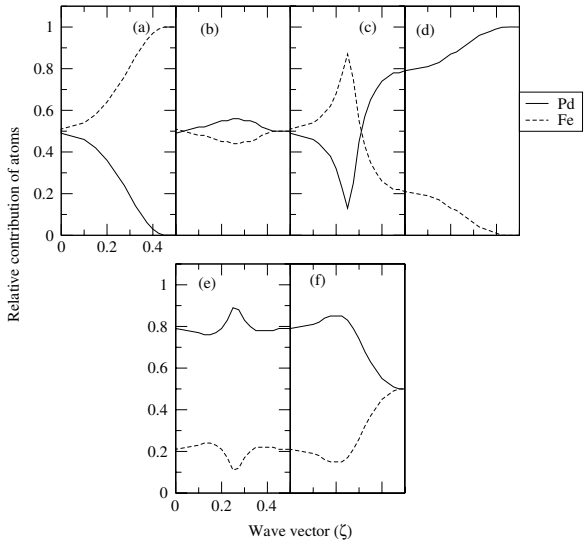

Figure 4. Relative contribution of Fe and Pd towards each mode along [$\zeta\zeta\zeta$] in FePd. Parts (a)–(f) refer to modes 1–6, respectively, in figure 1.

in frequency. The theoretically calculated frequencies in general agree well with the experimental ones with maximum deviation being observed for the high frequency LO modes along [ζ00]. Once again we find the theoretical values to be higher than the experimental ones as was observed for FePd. The calculated densities of states agree better with the experimental one than in the FePd case. The peak with the highest intensity is observed around 4 THz and the small peaks around 6 THz observed experimentally are also observed in our calculations. However, the sharp peak around 5 THz observed experimentally manifests itself as a flat plateau in our calculations. As expected, Pd atoms contribute most to the densities of states throughout the frequency spectrum, a feature also observed in the experimentally obtained curve.

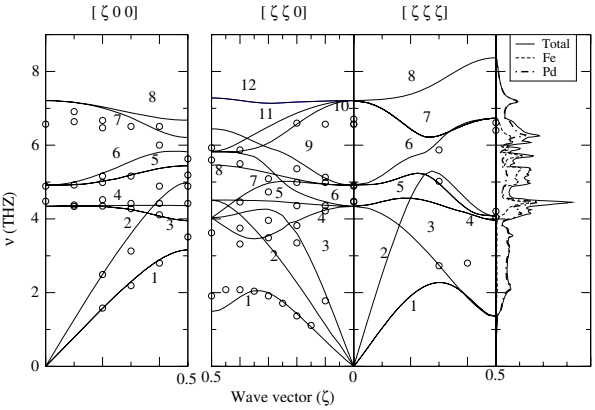

Figure 5. Dispersion curves (frequency ν versus reduced wavevector ζ) and phonon densities of states (partial and total) for $FePd_3$ alloy. The open circles are the experimental data [13].

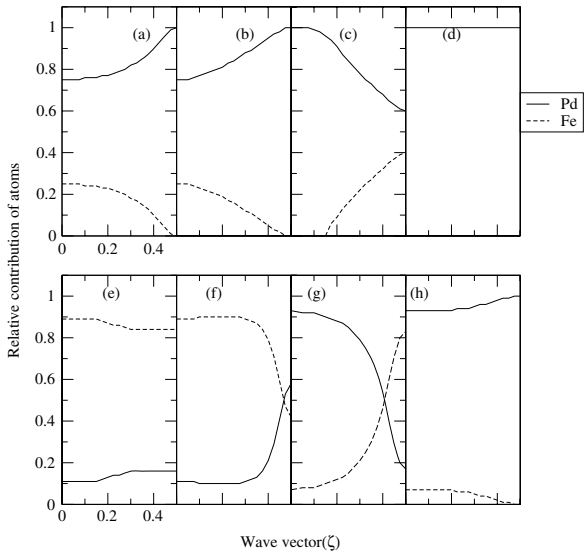

Figure 6. Relative contribution of Fe and Pd to each mode along $[\zeta 00]$ in $FePd_3$. Parts (a)–(h) refer to modes 1–8, respectively, in figure 5.

In figures 6–8 we show the atom-specific contributions to each mode along the three symmetry directions. For all three symmetry directions, we see that the Pd atoms contribute more towards most of the modes. The modes which are Fe dominated (modes 5 and 6 along $[\zeta 00]$, modes 6, 8 and 9 along $[\zeta\zeta 0]$ and modes 2 and 6 along $[\zeta\zeta\zeta]$) are mostly in the middle of the spectrum, i.e. in the frequency range 4–6 THz. This correlates with the observed fact that the contribution of Fe to densities of states is significant in this frequency range only.

3.3. Force constants

In order to find out the correlation between *ab initio* frequencies being larger than the experimental ones, the difference in experimentally and theoretically obtained densities of states and the overwhelming Pd contribution for the entire range of frequencies, particularly in $L1_0$ FePd, we look at the force constants between various pairs of atoms

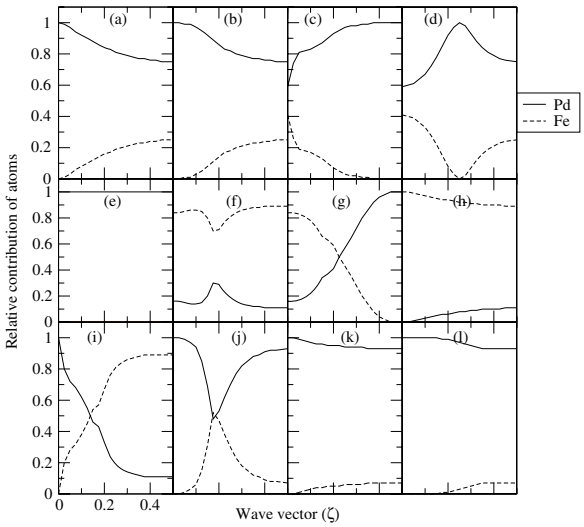

Figure 7. Relative contribution of Fe and Pd to each mode along $[\zeta\zeta 0]$ in $FePd_3$. Parts (a)–(l) refer to modes 1–12, respectively, in figure 5.

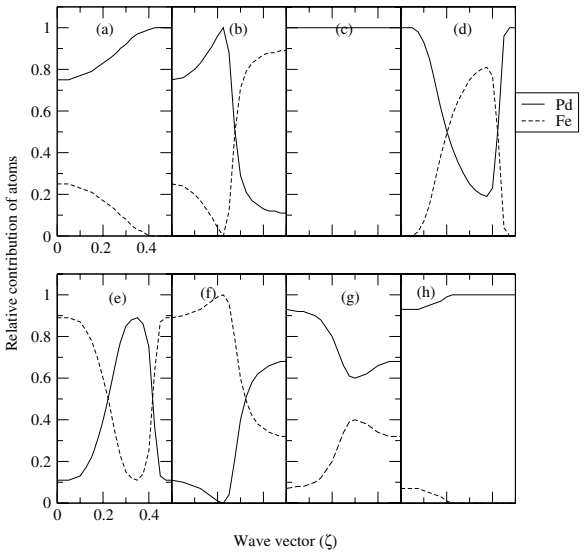

Figure 8. Relative contribution of Fe and Pd to each mode along $[\zeta\zeta\zeta]$ in $FePd_3$. Parts (a)–(h) refer to modes 1–8, respectively, in figure 5.

obtained in *ab initio* calculations and compare them with the experimental force constants which are obtained by fitting the frequencies to the Born–Von Karman force constant model. To make a direct comparison between theory and experiment, we converted the *ab initio* force constant matrix to one containing only longitudinal and transverse components. To do this, we aligned the z-axis along the line connecting the atoms in question and performed a basis transformation. The transverse components were averaged. Since the higher neighbor force constants are an order of magnitude smaller than the nearest-neighbor ones, we consider the nearest-neighbor ones only. In table 1, Pd–Pd nearest-neighbor force constants in FePd and $FePd_3$ are given. For comparison, we have also calculated the force constants of pure fcc Pd. The *ab initio* Pd–Pd force

Table 1. Pd–Pd nearest-neighbor force constants in N m^{-1}. L is the longitudinal and T is the transverse component of force constant.

System	Bond distance (au)	L (this calc.)	T (this calc.)	L (Expt)	T (Expt)
Pd	5.189	52.1	−3.0	42.9[a]	−2.5[a]
$FePd_3$	5.150	60.4	−3.5	54.2[b]	−2.3[b]
FePd	5.154	66.3	−4.7	52.1[c]	−2.7[c]

[a] Reference [25].
[b] Reference [13].
[c] Reference [14].

Table 2. Fe–Fe nearest-neighbor force constants in N m^{-1}. L is the longitudinal and T is the transverse component of force constant.

System	Bond distance (au)	L (this calc.)	T (this calc.)	L (Expt)	T (Expt)
$FePd_3$	—	—	—	—	—
FePd	5.154	11.3	−2.6	21.3[a]	−1.6[a]

[a] Reference [14].

constants in general are much higher than the experimental ones. The interesting feature is that in spite the bond distances of Pd atoms in FePd and $FePd_3$ being almost identical the longitudinal force constants differ significantly. Although the experimental ones differ by 3% only, the theoretical ones differ by 10%. The longitudinal components should also increase with decreasing bond distance because this component is associated with stretching of the particular bond. If the bond distance decreases, the relevant bonds stiffen, resulting in a higher value of the longitudinal component of the force constant. The *ab initio* results follow this trend correctly. However, the 10% increase of the longitudinal component in FePd over that in $FePd_3$ can be explained by looking at the volume per atom available. While volume per atom in $FePd_3$ is 96.656 au^3, it is 93.949 au^3 in FePd. Therefore, in FePd, the bigger Pd atoms have about 3% less volume available which stiffens the Pd–Pd interaction in comparison to that in $FePd_3$. In table 2, the force constants between Fe–Fe nearest neighbors are given. Since $FePd_3$ does not have any Fe as nearest neighbors of Fe atoms, we provide data for FePd only. The *ab initio* force constants are much softer than that obtained from experiments. This feature can explain the reason behind the overwhelming domination of Pd atoms in the system. The *ab initio* Fe–Fe interactions are too weak to contribute significantly to the lattice dynamics, and therefore the densities of states are dominated by Pd throughout the spectrum. In table 3 we present a comparison of Fe–Pd nearest-neighbor force constants. The agreement between experiment and theory in this case is better, and both follow the expected trend of stiffening of bonds with decreasing bond distances. The Fe–Pd bonds calculated by theory are softer than those obtained from experiments as was seen in the case of Fe–Fe bonds as well.

Analyzing the trends in the force constants between various pairs of species, we find that the disagreement between the *ab initio* and experimental results is due to too much stiffening of Pd–Pd bonds and too much softening of Fe–Fe bonds. This can be due to the choice of lattice constant and the exchange–correlation functional for *ab initio* calculations. For spin-polarized Fe and Ni, it has been observed that using experimental lattice constants and the GGA exchange–correlation functional produces frequencies larger than that of the experiment [23]. Although no results on *ab initio* force constants have been presented for these systems, the overestimation of frequencies can be correlated to the stiffening of bonds. Although GGA functionals act as a negative pressure on the system, thereby reducing the hardness of bonds in comparison to the LDA functionals, using a volume which is not the GGA equilibrium volume could result in the behavior observed in this work. The dependence of bond stiffness on the exchange correlation functional for these intermetallics should therefore be considered for future investigations.

Table 3. Fe–Pd nearest-neighbor force constants in N m^{-1}. L is the longitudinal and T is the transverse component of force constant.

System	Bond distance (au)	L (this calc.)	T (this calc.)	L (Expt)	T (Expt)
$FePd_3$	5.150	18.9	−0.9	23.6[a]	−0.8[a]
FePd	5.00	32.0	−0.6	34.3[b]	−2.1[b]

[a] Reference [13].
[b] Reference [14].

4. Conclusions

We have investigated the lattice dynamics of FePd and $FePd_3$ intermetallics using first-principles density functional perturbation theory. The agreement between our calculations an the results of neutron scattering experiments is fairly good except for some overestimation of first-principles frequencies. The densities of states curves for $FePd_3$ are in good agreement with the experiment but there are significant difference for FePd. We attribute these differences to the overwhelming stiffening of Pd–Pd bonds and subsequent softening of Fe–Fe bonds. The reason behind this could be the combination of the lattice constant and the exchange–correlation functional chosen in this work. In a future communication, we will investigate this point. Another interesting aspect worth investigating is the effect of magnetism on lattice dynamics. Very little information on this is available as far as first-principles calculations are concerned. It is a well-known fact that magnetism affects the lattice constants and therefore bond lengths. Since we have already observed that the force constants are strongly dependent upon bond lengths between a particular pair of species, it is worth investigating how the force constants alter as one changes the magnetic order. However, in this communication our motivation was to understand and compare the lattice dynamics with the change of composition of one component of the alloy. Hence we have restricted ourselves to the ground states of these systems which are ferromagnetic. Investigation of the effect of magnetism on the phonon spectrum will be taken up in the near future.

The results have been analyzed from the nearest-neighbor force constant values between various pairs of species. The behavior of *ab initio* force constant versus bond distance follows the expected trend. This is important from the point of view of feasibility of using *ab initio* ordered alloy force constants to study the disordered phases of FePd. Cedar and co-workers have shown [24] that the bond stiffness versus bond distance relationship is transferable across various environments and chemical compositions. This idea can be exploited for this system too. Experimental results for $Pd_{90}Fe_{10}$, $Pd_{72}Fe_{28}$ and $Pd_{50}Fe_{50}$ are available and awaiting microscopic interpretation. The results of this work can be useful to obtain the real picture of interplay of forces between various pairs of atoms in a disordered environment.

References

[1] Tanaka K, Ichitsubo T and Koiwa M 2001 *Mater. Sci. Eng.* A **312** 118
[2] Tanaka K and Moroika K 2003 *Phil. Mag.* A **83** 1797
[3] Harp G R, Weller D, Rabedeau T A, Farrow R F C and Toney M F 1993 *Phys. Rev. Lett.* **71** 2493
Cebollada A, Weller D, Sticht J, Harp G R, Farrow R F C, Marks R F, Savoy R and Scott J C 1994 *Phys. Rev.* B **50** 3419
[4] Weller D, Brandle H and Chappert C 1993 *J. Magn. Magn. Mater.* **121** 461
[5] Ersen O, Parasote V, Pierron-Bohnes V, Cadeville M C and Ulhaq-Bouillet C 2003 *J. Appl. Phys.* **93** 2987
[6] Parkin S, Jiang X, Kaiser C, Panchula A, Roche K and Samant M 2003 *Proc. IEEE* **91** 661
[7] Sanyal B, Bergqvist and Eriksson O 2003 *Phys. Rev.* B **68** 054417
[8] Bruesch P 1982 *Phonon, Theory and Experiment* (New York: Springer)
[9] Gehanno V, Marty A, Giles B and Samson Y 1997 *Phys. Rev.* B **55** 12552
[10] Kamp P, Marty A, Giles B, Hoffman R, Marchesini S, Belakhovsky M, Boeglin C, Durr H A, Dhesi S S, Van der Laan G and Rogalev A 1999 *Phys. Rev.* B **59** 1105
[11] Maliszewski E, Sosnowski J, Bednarski S, Czachor A and Holas A 1975 *J. Phys. F: Met. Phys.* **5** 1455
[12] Sato M, Grier B H, Shapiro S M and Miyajima H 1982 *J. Phys. F: Met. Phys.* **12** 2117
[13] Stirling W G, Cowley R A and Stringfellow M W 1972 *J. Phys. F: Met. Phys.* **2** 421
[14] Mehaddene T, Kentzinger E, Hennion B, Tanaka K, Numakura H, Marty A, Parasote V, Cadeville M C, Zemirli M and Pierron-Bohnes V 2004 *Phys. Rev.* B **69** 024304
[15] Singh N 1990 *Phys. Rev.* B **42** 8882
Akgun I and Ugur G 1995 *Phys. Rev.* B **51** 3458
[16] Baroni S, De Gironcoli S, Dal Corso A and Giannozzi P 2001 *Rev. Mod. Phys.* **73** 515
[17] Pickett W 1989 *Comput. Phys. Rep.* **9** 115
[18] Louie S G, Froyen S and Cohen M L 1982 *Phys. Rev.* B **26** 1738
[19] Perdew J P, Burke K and Ernzerhof M 1996 *Phys. Rev. Lett.* **77** 3865
[20] Methfessel M and Paxton A T 1989 *Phys. Rev.* B **40** 3616
[21] Giannozzi P, De Gironcoli S, Pavone P and Baroni S 1991 *Phys. Rev.* B **43** 7231
[22] Gilat G and Raubenheimer L J 1966 *Phys. Rev.* **144** 390
[23] Dal Carso A and De Gironcoli S 2000 *Phys. Rev.* B **62** 273
[24] Van De Walle A and Cedar G 2000 *Phys. Rev.* B **61** 5972
[25] Miller A P and Brockhouse B N 1968 *Phys. Rev. Lett.* **20** 798